Electronic Supplementary Material (ESI) for RSC Advances.

Electronic Supplementary Information

Correlating the Surface Structure and Hydration of γ-Al_2O_3 Support with the Ru_n (n=1-4) Clusters Adsorption Behavior: A Density Functional Theory Study

J. Yang,[a] H. Wang,[b] X. Zhao,[b] Y. L. Li[b] and W.L. Fan[a]*

[a] Key Laboratory for Colloid and Interface Chemistry of State Educating Ministry, School of Chemistry and Chemical Engineering, Shandong University, Jinan 250100, China. Fax: +86-531-88364864; Tel: +86-531-88366330; E-mail: fwl@sdu.edu.cn

[b] State Key Laboratory of Crystal Materials, Shandong University, Jinan 250100, China

Financial support from the National Natural Science Foundation of China (Grant no.: 21173131) and the Taishan Scholar Project of Shandong Province is gratefully acknowledged.

1. The choice for the computation details:

The convergence test in Figure S1 showed the change of bulk energy became very few from the 340 eV. In other words, the 340 eV was suitable for conducting the computation.

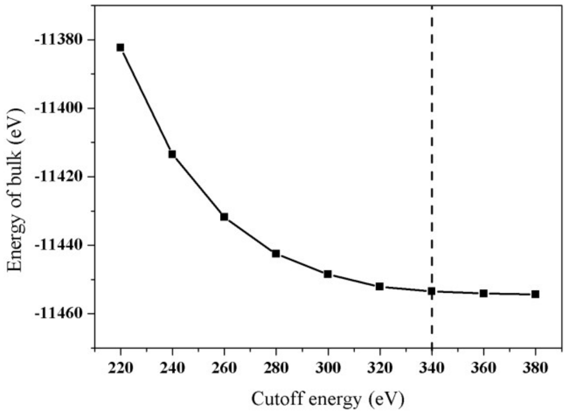

Figure S1. The convergence test for cutoff energy of the slab.

2. The test for the slab model

(1) The test for vacuum thickness

Based on the data in Figure S2, the surface energy became very few from the 12 Å, indicating the vacuum thickness chosen to 12 Å was long enough to shield the self-interaction of the periodic boundary conditions.

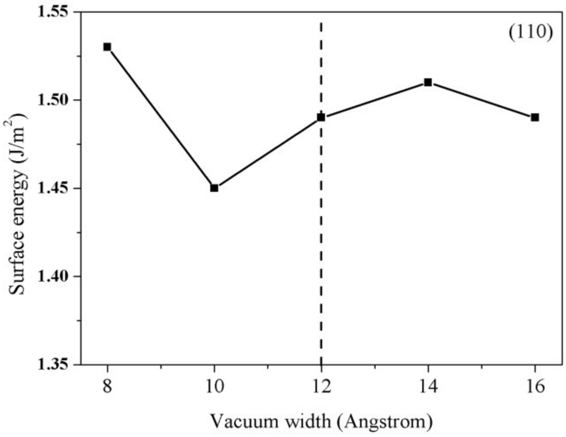

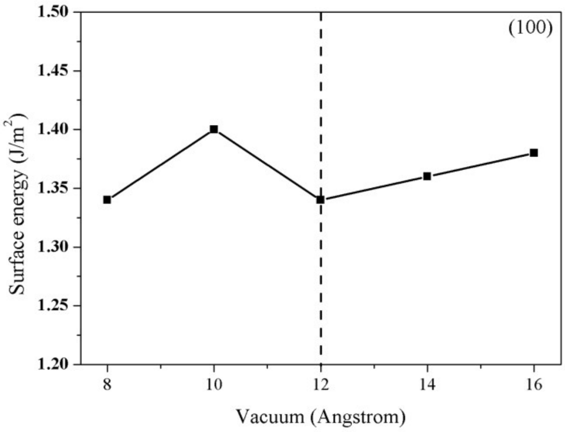

Figure S2. The convergence tests for the thickness of vacuum slab on the (100) and (110) surfaces.

(2) The choice of the slab terminations:

As presented in Figure S3, the (110) and (100) surface have different terminations: the O_{4c}-Al_{3c}-$2O_{2c}$, O_{2c}-Al_{3c}-$2O_{3c}$ or O_{4c}-Al_{3c}-$2O_{3c}$ terminations on (110) and Al_{5c} or Al_{2c} terminations on (100) surfaces. A comparison of surface energies indicates that O_{4c}-Al_{3c}-$2O_{2c}$ terminated (110) and Al_{5c} terminated (100) have much lower surface energies than others (as is shown in Table S1).

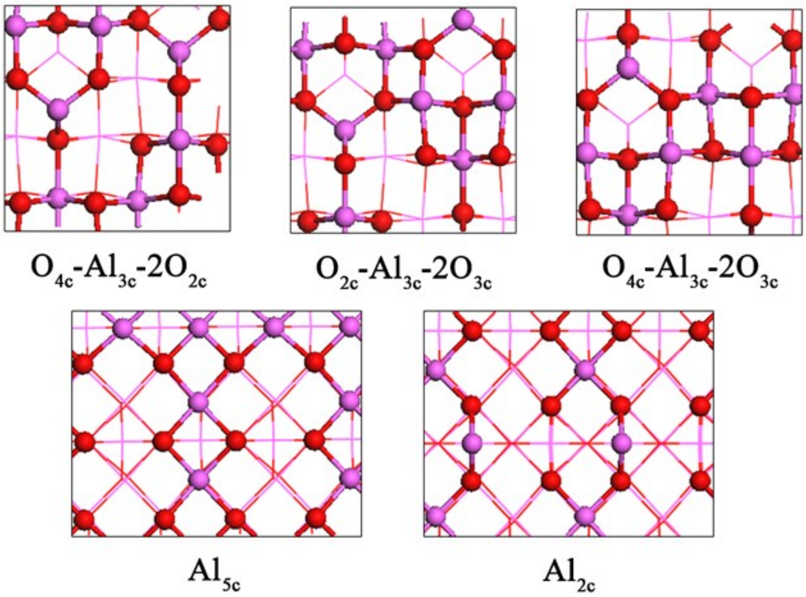

FigureS3. Top views of (110) and (100) surface with different terminations.

Table S1. The surface energies of (110) and (100) surface with different terminations.

Surface plane	Terminations	Surface energy (J/m^2)
(110)	O_{4c}-Al_{3c}-$2O_{2c}$	1.42
	O_{2c}-Al_{3c}-$2O_{3c}$	1.45
	O_{4c}-Al_{3c}-$2O_{3c}$	1.65
(100)	Al_{5c}	0.92
	Al_{2c}	1.64

3. The potential energy profiles for the dissociation of H_2O on dehydrated (110) and (100) surfaces

The transition states for possible dissociation states of H_2O on (110) and (100) surface was tested (Table S2). It can be found dissociation of H_2O at Al_{3c}-O_{2c3} site is more preferred than that at Al_{4c}-O_{2c1} site. Moreover, the dissociation process of water across the Al_{5c2}-O_b site with an activation energy of 1.74 eV is more exothermic than that on others. The reaction transition states, intermediates and products involved in are shown in Figure S4 and Figure S5.

Table S2. The activation energy (Ea), reaction energy (△E) for the hydroxylation process the(110) and (100) surfaces.

（110）	Al3c-O2c3	Al4c-O2c1		
Ea (eV)	0.70	0.62		
△E (eV)	-1.06	-0.31		
（100）	Al5c2-Ob	Al5c2-Oa	Al5c1-Oc	Al5c1-Oa
Ea (eV)	1.74	2.32	1.79	2.40
△E (eV)	-0.35	1.28	0.78	1.35

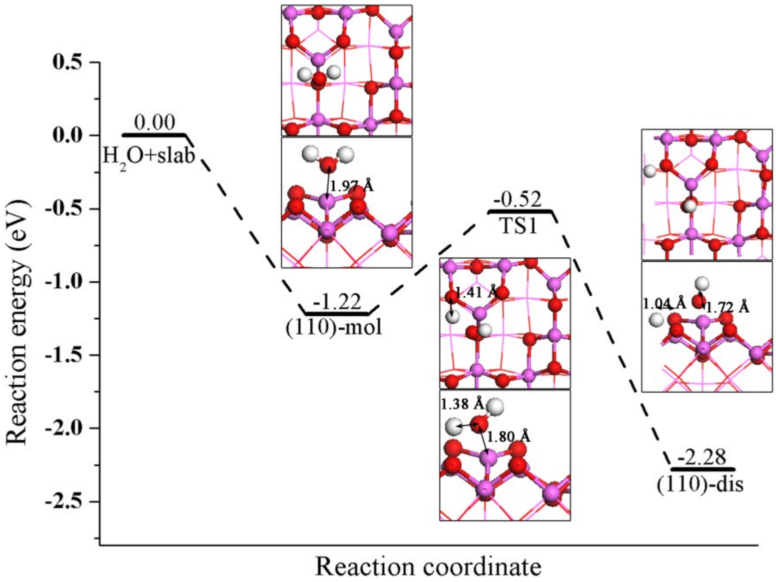

Figure S4. The potential energy profile for H_2O dissociation on the dehydrated (110) surface. Structures of the initial, transition and final states are included.

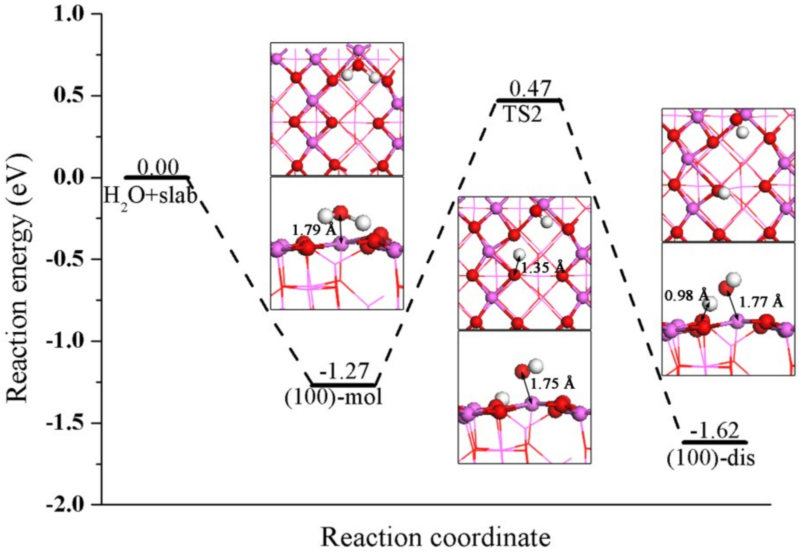

Figure S5. The potential energy profile for H_2O dissociation on the dehydrated (100) surface. Structures of the initial, transition and final states are included.

4. The optimized configurations for less stable adsorption

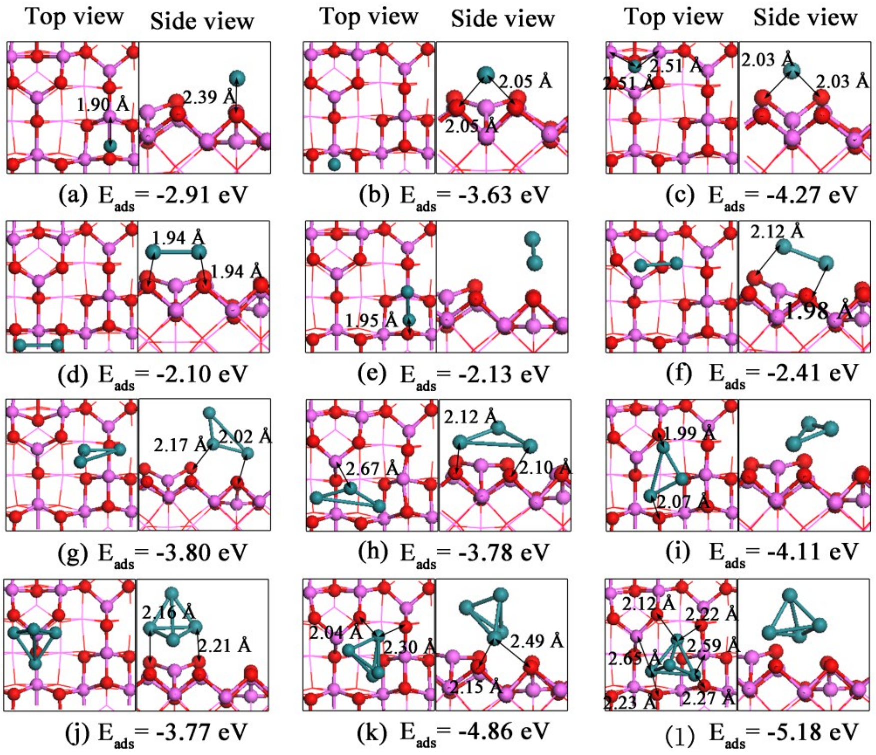

(a) E_{ads}= -2.91 eV (b) E_{ads}= -3.63 eV (c) E_{ads}= -4.27 eV

(d) E_{ads}= -2.10 eV (e) E_{ads}= -2.13 eV (f) E_{ads}= -2.41 eV

(g) E_{ads}= -3.80 eV (h) E_{ads}= -3.78 eV (i) E_{ads}= -4.11 eV

(j) E_{ads}= -3.77 eV (k) E_{ads}= -4.86 eV (1) E_{ads}= -5.18 eV

Figure S6. The possible adsorption states for Ru_n (n=1-4) clusters on dehydrated (110) surface.

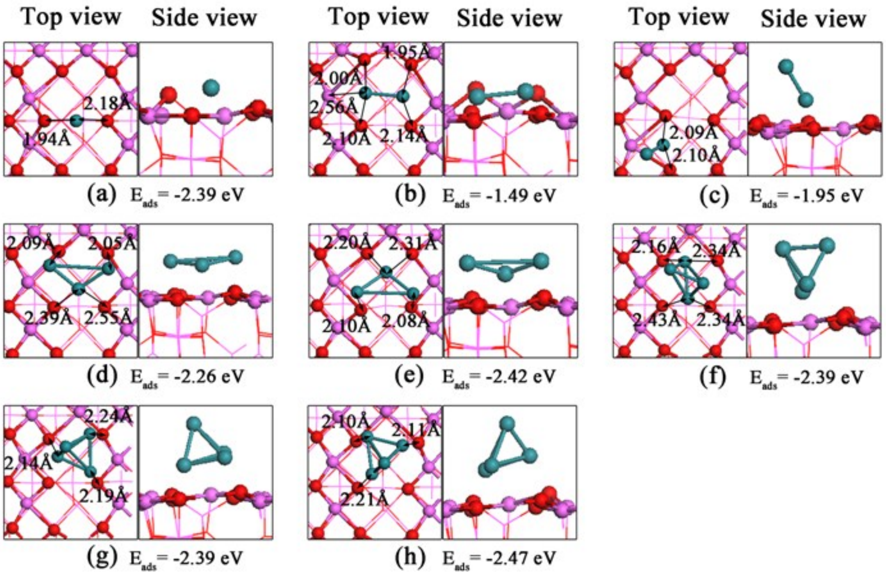

(a) E_{ads}= -2.39 eV (b) E_{ads}= -1.49 eV (c) E_{ads}= -1.95 eV

(d) E_{ads}= -2.26 eV (e) E_{ads}= -2.42 eV (f) E_{ads}= -2.39 eV

(g) E_{ads}= -2.39 eV (h) E_{ads}= -2.47 eV

Figure S7. The possible adsorption states for Ru_n (n=1-4) clusters on dehydrated (100) surface.

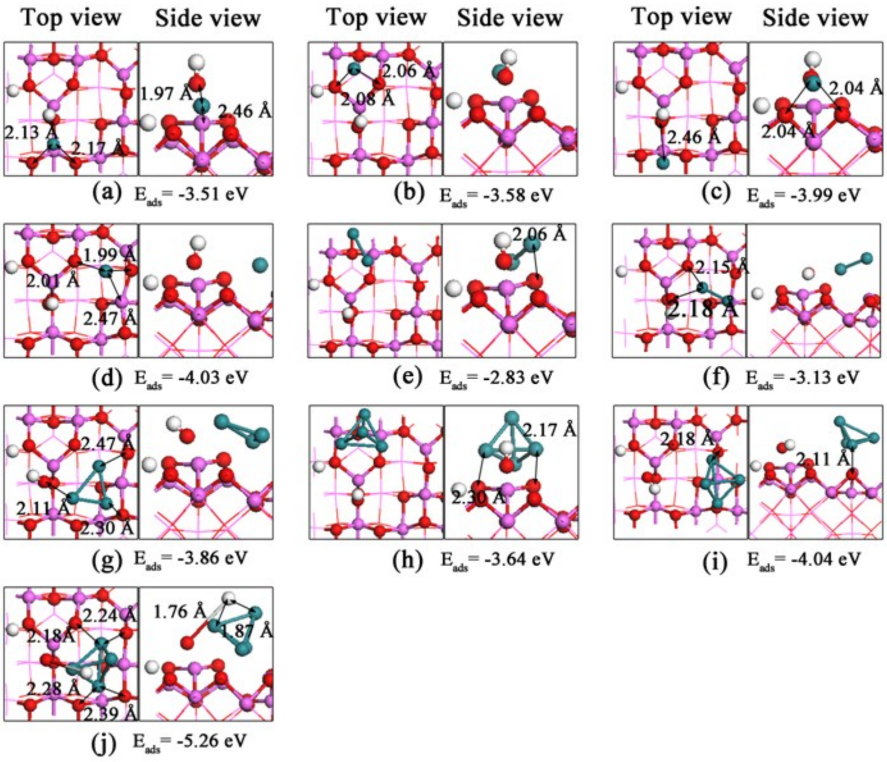

Figure S8. The possible adsorption states for Ru_n (n=1-4) clusters on hydrated (110) surface.

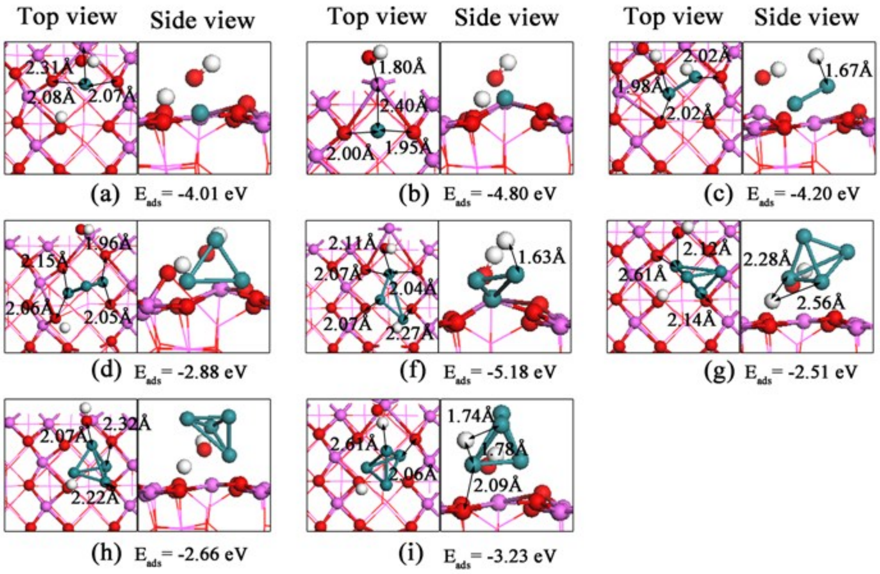

Figure S9. The possible adsorption states for Ru_n (n=1-4) clusters on hydrated (100) surface.

5. The effect of spin-polarized on adsorption

The spin-polarized calculations are performed on favorable configurations of Ru_n (n=1-4) clusters adsorption. Comparing the adsorption energy of each configuration spin-restricted and spin–unrestricted (Table S3), we can see the difference between them is within 0.01-0.22 eV, comprising few percent of the adsorption energies. Furthermore, population analysis (as shown in Table S4-7) based on spin-unrestricted indicates the Ru_n cluster- support interaction is similar to back-donation interaction, where Ru and O atom is charge deficit and Al atom is charge abundant. Calculations show that the spin-polarize induces subtle variation of Mulliken charge for involved sites (less than 0.08 |e|). This means that the spin-polarized of Ru_n cluster has little effect on the adsorption energies and charge transfer for Ru_n cluster adsorption on Al_2O_3 support.

Table S3. The adsorption energies of most stable configurations for spin-restricted and spin-unrestricted Ru_n (n=1-4) clusters on dehydrated and hydrated γ-Al_2O_3 (110) and (100) surfaces

surface		E_{ads} (eV)			
		Ru_1	Ru_2	Ru_3	Ru_4
D(110)	spin-restricted	-4.33	-3.76	-4.73	-5.18
	spin-unrestricted	-4.44	-3.94	-4.89	-5.34
D(100)	spin-restricted	-4.62	-2.18	-3.66	-3.31
	spin-unrestricted	-4.71	-2.11	-3.78	-3.23
H(110)	spin-restricted	-4.39	-3.22	-4.18	-4.48
	spin-unrestricted	-4.34	-3.44	-4.36	-4.58
H(100)	spin-restricted	-4.71	-3.14	-4.26	-3.69/-3.63
	spin-unrestricted	-4.70	-3.10	-4.15	-3.87/-3.65

Table S4. Mulliken charges of spin-restricted and spin-unrestricted Ru_n (n=1-4) adsorption in stable configurations on the dehydrated γ-Al_2O_3 (110) surface.

Mulliken charges, |e|	Ru_n	O_{2c1}	O_{2c2}	O_{3c1}	O_{3c2}	O_{3c3}	Al_{3c}	Al_{4c}
D(110)		-1.17	-1.16	-1.12	-1.13	-1.13	1.78	1.79
D(110)-1a	0.29	-0.99	-1.04	-1.11	-1.13	-1.13	1.74	1.41
D(110)-2a	0.33	-1.07	-1.02	-1.10	-1.01	-1.10	1.38	1.50
D(110)-3	0.38	-1.12	-1.02	-0.97	-0.99	-1.08	1.36	1.41
D(110)-4	0.46	-1.02	-1.03	-1.00	-1.01	-1.10	1.36	1.40

Table S5. Mulliken charges of spin-restricted and spin-unrestricted Ru_n (n=1-4) adsorption in stable configurations on the dehydrated γ-Al_2O_3 (100) surface.

Mulliken charges, |e|	Ru_n	O_a	O_b	O_c	O_d	O_E	Al_{5c1}	Al_{5c2}	Al_{5c3}
D(100)	-	-1.17	-1.11	-1.11	-1.07	-1.10	1.70	1.65	1.66
D(100)-1	0.09	-1.15	-1.10	-1.00	-0.97	-1.10	1.67	1.31	1.64
D(100)-2	0.19	-1.14	-1.03	-0.99	-0.96	-1.14	1.65	1.29	1.68
D(100)-3	0.02	-1.15	-0.96	-0.99	-0.94	-1.12	1.50	1.36	1.66
D(100)-4	0.16	-1.15	-0.98	-1.00	-1.01	-1.04	1.52	1.35	1.48

Table S6. Mulliken charges of spin-restricted and spin-unrestricted Ru_n (n=1-4) adsorption in stable configurations on the hydrated γ-Al_2O_3 (110) surface.

Mulliken charges, |e|	Ru_n	O_{2c1}	O_{2c2}	O_{3c1}	O_{3c2}	O_w	Al_{3c}	Al_{4c}
H(110)		-1.14	-1.20	-1.12	-1.13	-1.13	1.85	1.80
H(110)-1	0.30	-1.13	-1.18	-1.06	-1.00	-0.96	1.80	1.37
H(110)-2	0.36	-1.06	-1.06	-1.10	-0.99	-0.93	1.68	1.36
H(110)-3	0.28	-0.99	-1.07	-1.09	-1.01	-0.96	1.78	1.25
H(110)-4	0.34	-1.03	-1.06	-1.02	-1.01	-0.96	1.69	1.31

Table S7. Mulliken charges of spin-restricted and spin-unrestricted Ru_n (n=1-4) adsorption in stable configurations on the hydrated γ-Al_2O_3 (110) surface.

Mulliken charges, |e|	Ru_n	O_a	O_b	O_c	O_d	O_w	H_a	Al_{5c4}
H(100)		-1.17	-1.03	-1.12	-1.10	-1.11	0.48	1.68
H(100)-1	0.53	-1.06	-1.02	-1.01	-0.98	-1.04	-0.16	1.66
H(100)-2	0.57	-1.09	-0.99	-1.02	-1.07	-0.95	-0.20	1.68
H(100)-3	0.60	-1.05	-1.00	-0.96	-0.99	-0.94	-0.21	1.44
H(100)-4a	0.49	-1.05	-1.00	-1.04	-0.99	-0.96	-0.17	1.67
H(100)-4b	0.51	-1.06	-1.00	-1.00	-1.07	-0.93	-0.12	1.55

6. The charge density difference for different configurations

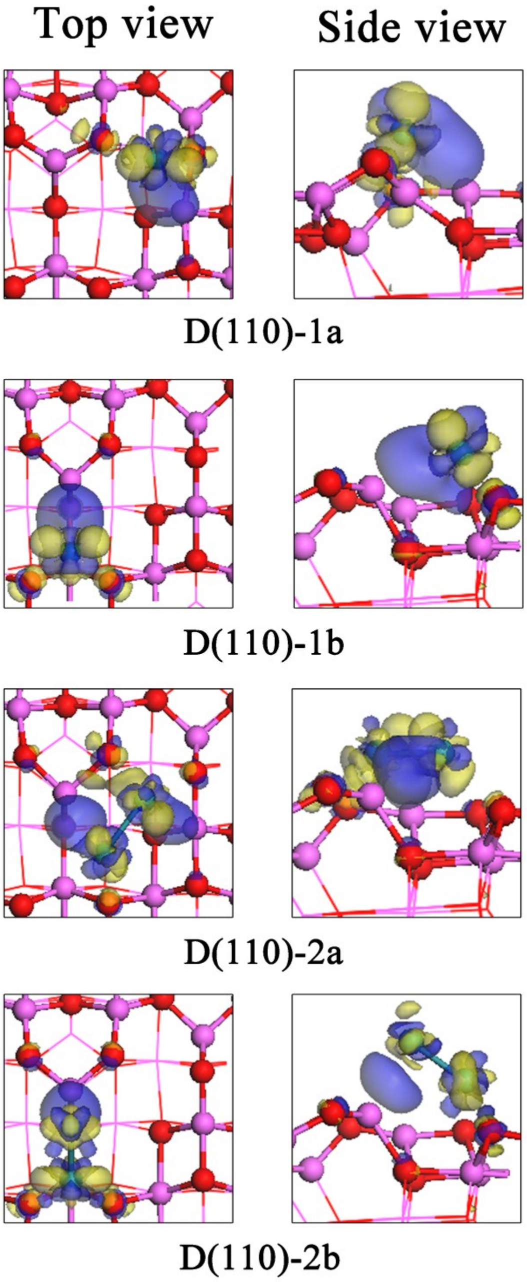

D(110)-1a

D(110)-1b

D(110)-2a

D(110)-2b

Figure S10. Charge density difference plots for Ru_n (n=1-2) clusters adsorption on dehydrated γ-Al_2O_3 (110) surface. The blue region indicates the electron density has been accumulated, conversely, the yellow region indicates the density has been depleted. The iso-surface is 0.05 electrons/ $Å^3$.

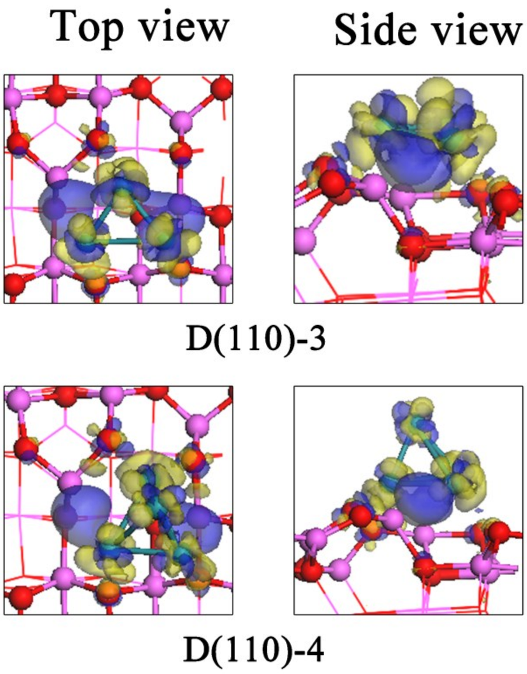

Figure S11. Charge density difference plots for Ru_n (n=3-4) clusters adsorption on dehydrated γ-Al_2O_3 (110) surface. The blue region indicates the electron density has been accumulated, conversely, the yellow region indicates the density has been depleted. The iso-surface is 0.05 electrons/ Å^3.

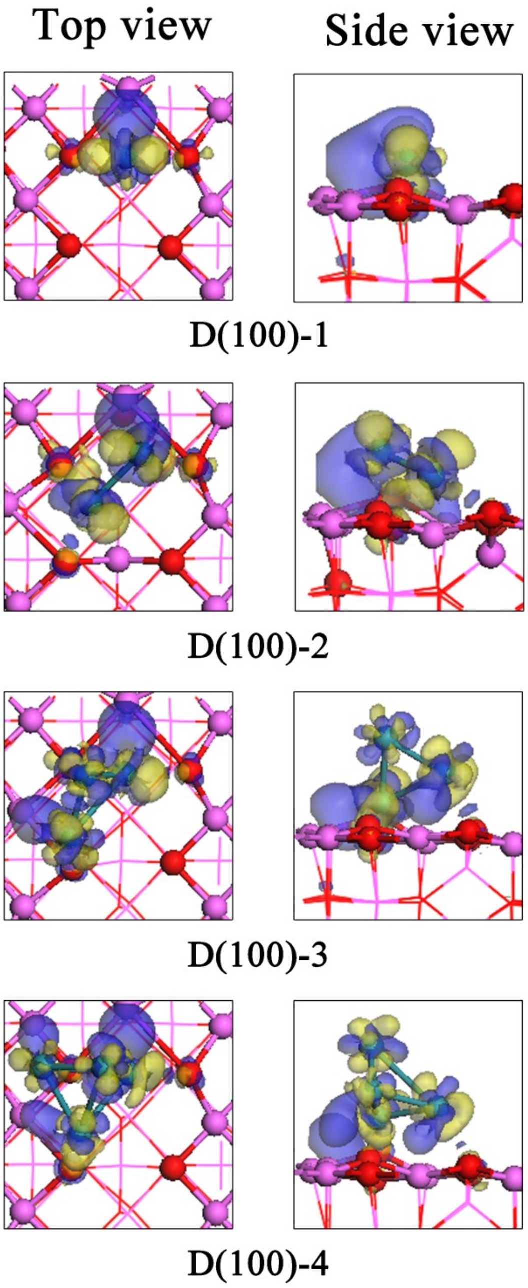

Figure S12.Charge density difference plots for Ru_n (n=1-4) clusters adsorption on dehydrated (100) surface. The blue region indicates the electron density has been enriched, conversely, the yellow region indicates the density has been depleted. The iso-surface is 0.05 electrons/ Å3.

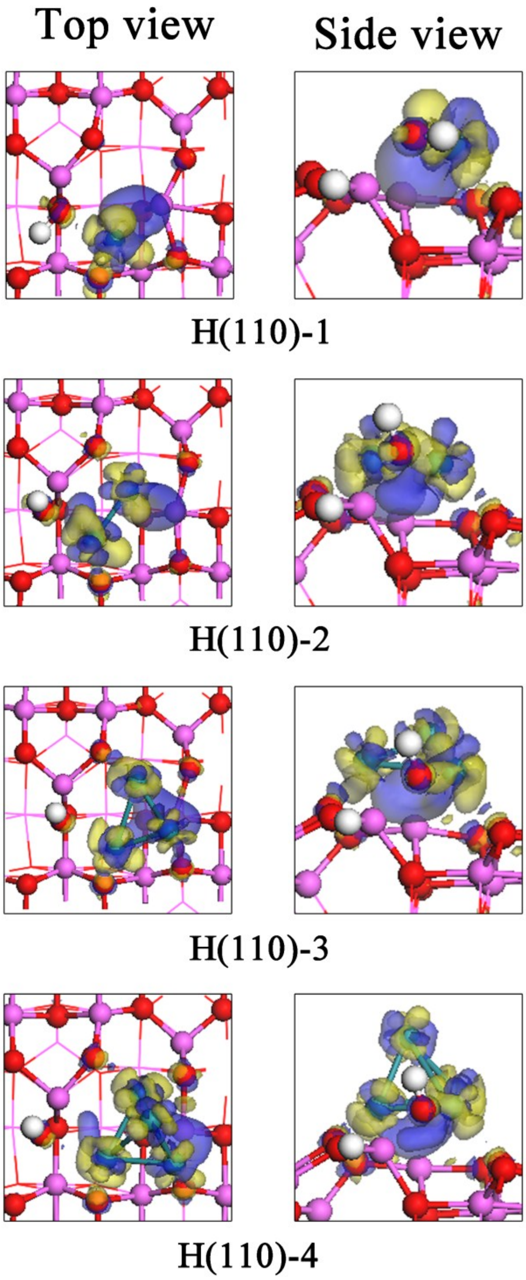

Figure S13.Charge density difference plots for Ru_n (n=1-4) clusters adsorption on hydrated (110) surface. The blue region indicates the electron density has been enriched, conversely, the yellow region indicates the density has been depleted. The iso-surface is 0.05 electrons/ $Å^3$.

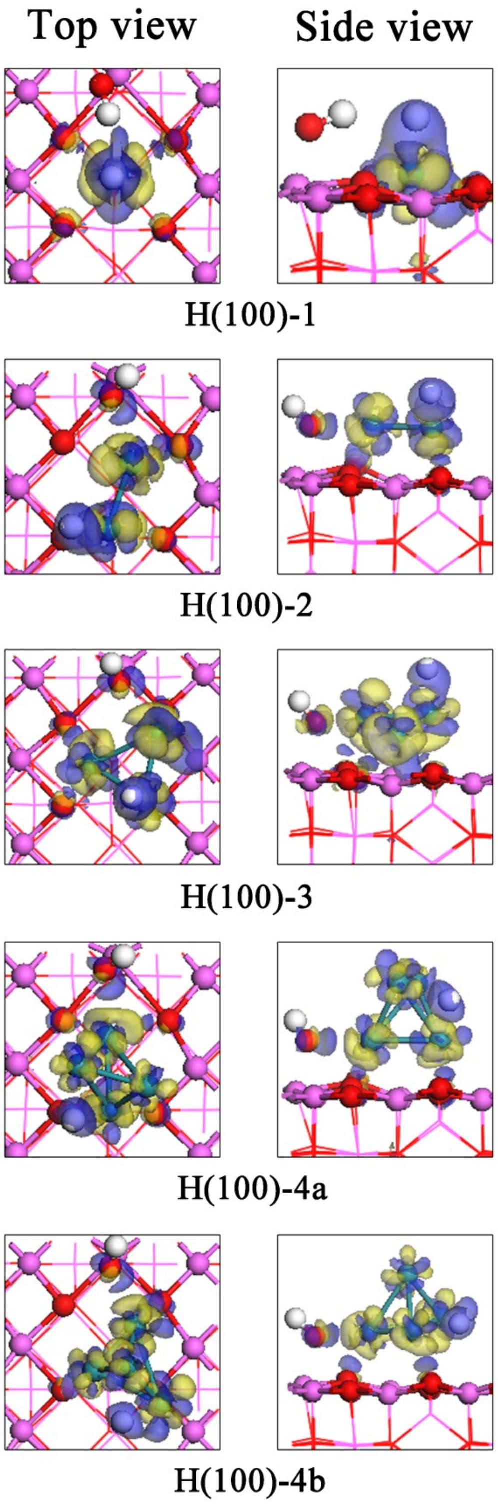

Figure S14. Charge density difference plots for Ru_n (n=1-4) clusters adsorption on hydrated (100) surface. The blue region indicates the electron density has been enriched, conversely, the yellow region indicates the density has been depleted. The iso-surface is 0.05 electrons/ Å^3.

7. The PDOS for atoms of different surfaces

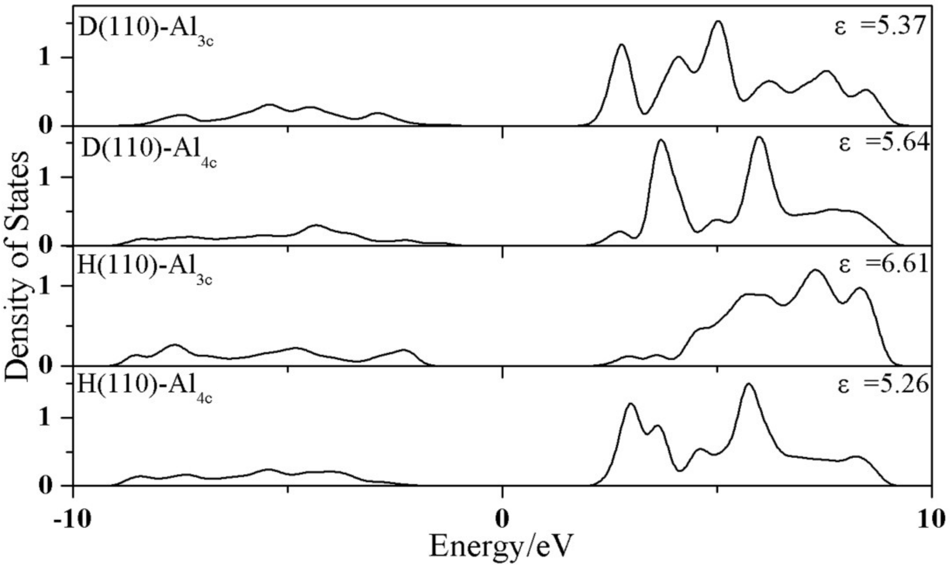

Figure S15. Project density of States (PDOS) for the Al atoms on the dehydrated (110) and hydrated (110) surface. The Fermi level was set at zero energy.

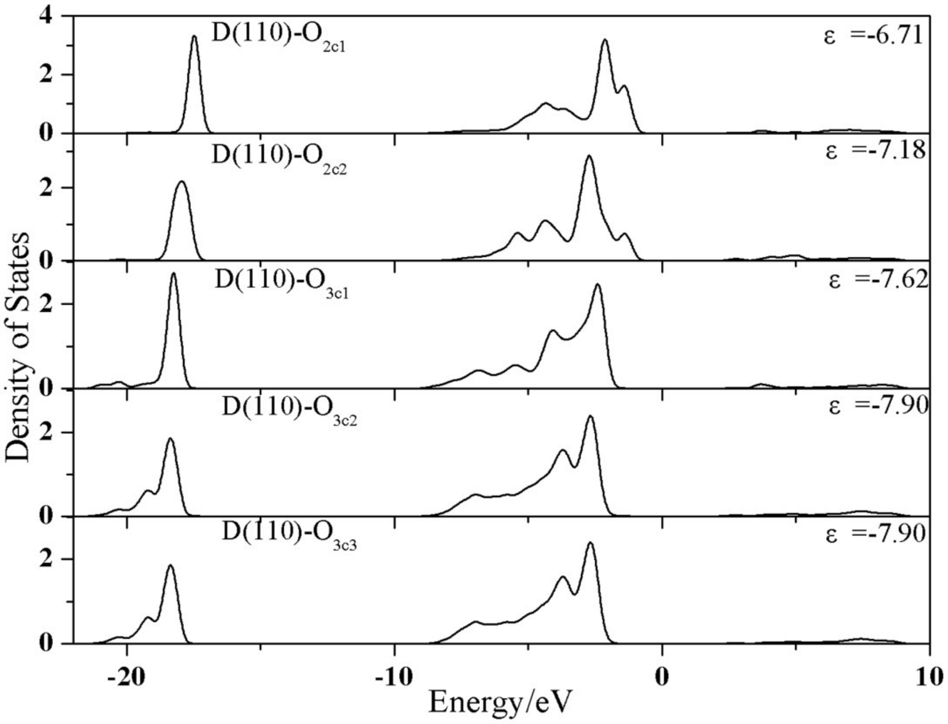

Figure S16. Project density of States (PDOS) for the O atoms on the dehydrated (110) surface. The Fermi level was set at zero energy.

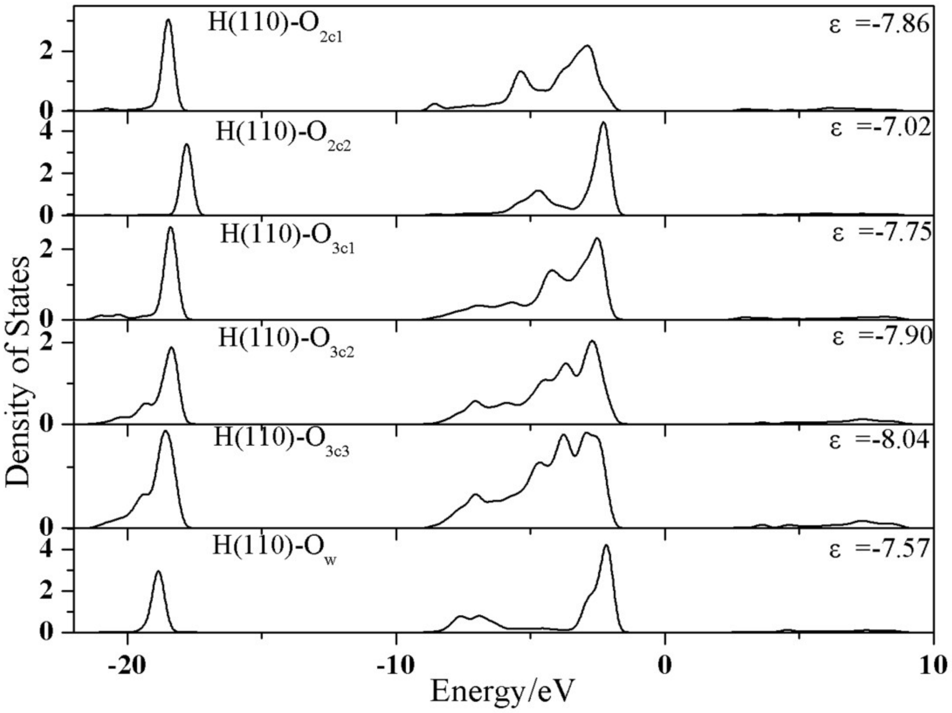

Figure S17. Project density of States (PDOS) for the O atoms on the hydrated (110) surface. The Fermi level was set at zero energy.

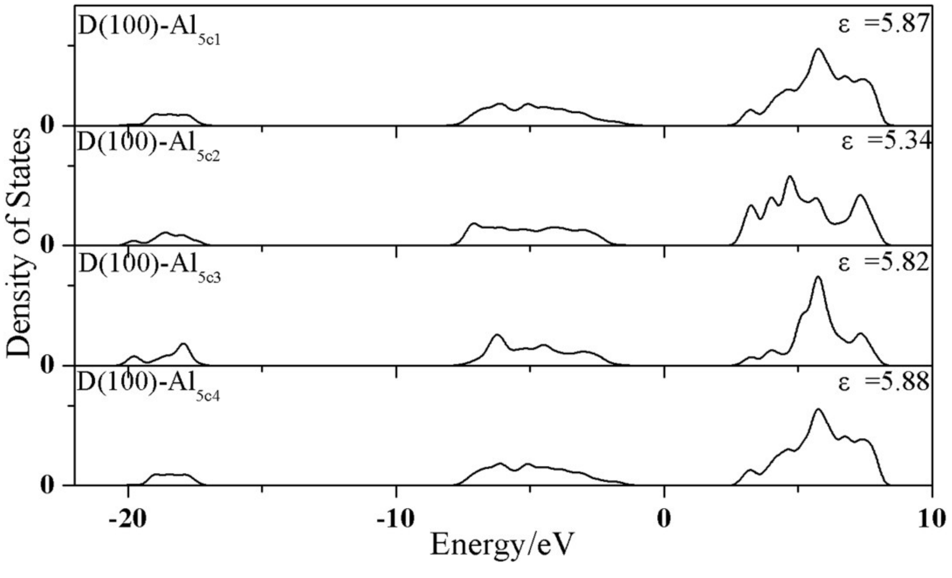

Figure S18. Project density of States (PDOS) for the Al atoms on the dehydrated (100) surface. The Fermi level was set at zero energy.

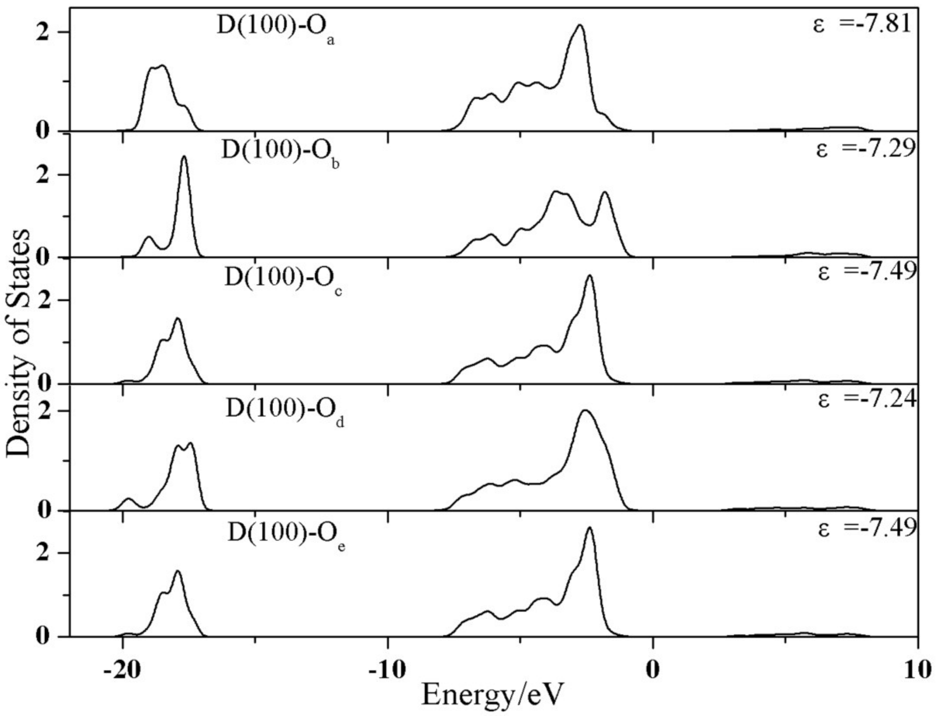

Figure S19. Project density of States (PDOS) for the O atoms on the dehydrated (100) surface. The Fermi level was set at zero energy.

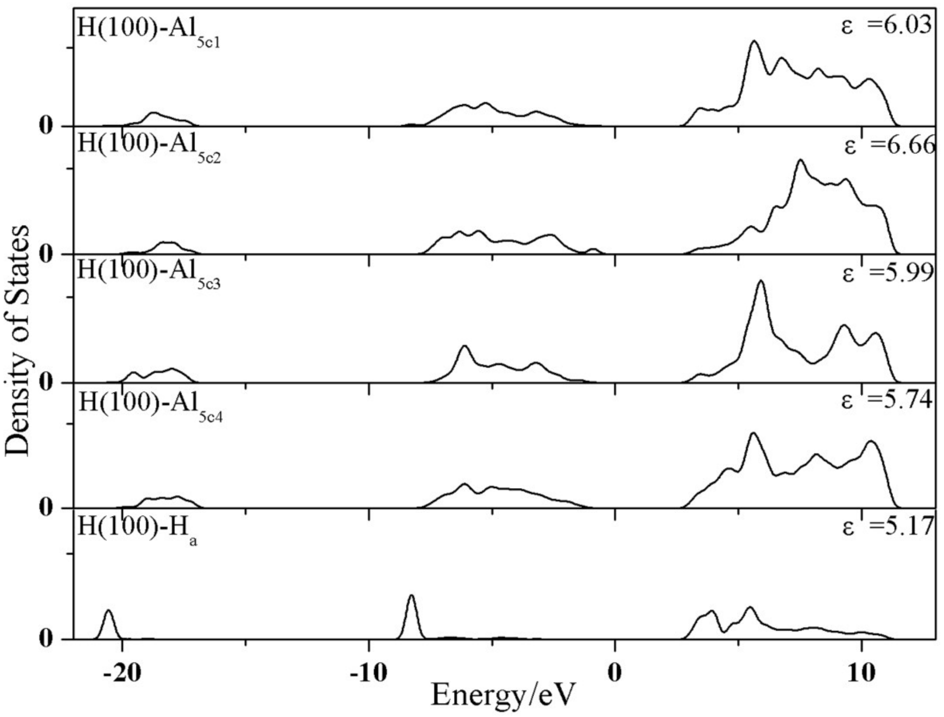

Figure S20. Project density of States (PDOS) for the Al atoms on the hydrated (100) surface. The Fermi level was set at zero energy.

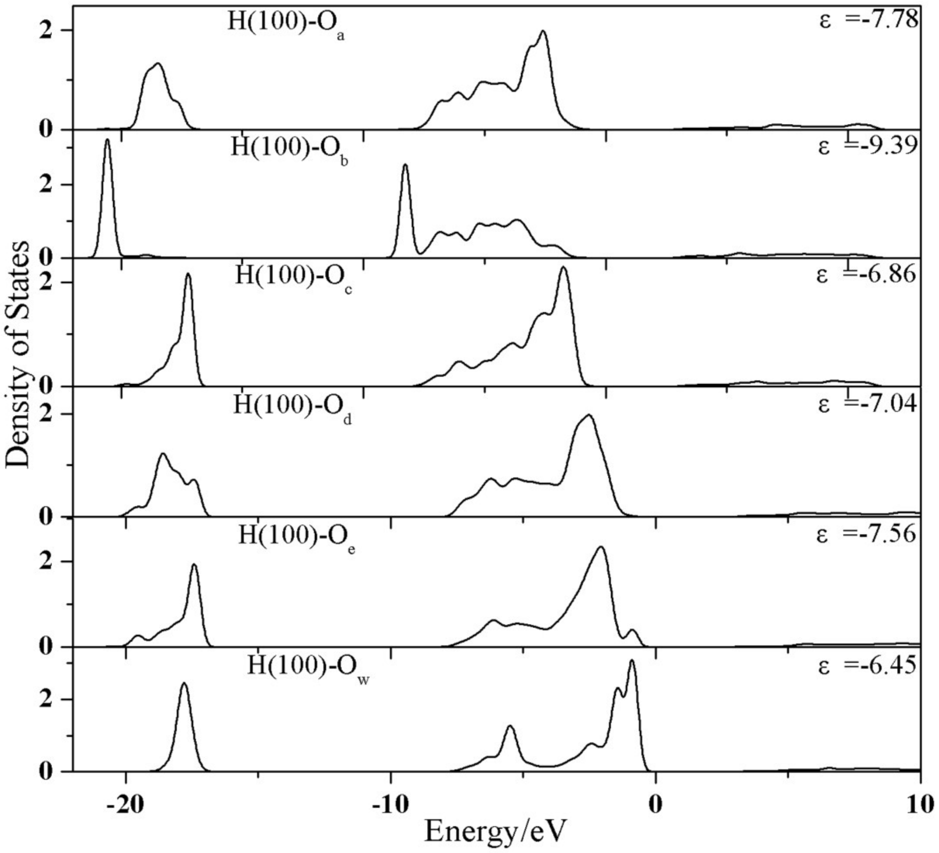

Figure S21. Project density of States (PDOS) for the O atoms on the hydrated (100) surface. The Fermi level was set at zero energy.

8. The relationship between (εAl - εO) values and interaction energies

We fit the interaction energy date to the following linear form

$$E_{int} = k\left(\varepsilon_{Al} - \varepsilon_{O}\right) + b$$

The results in Figure S22 clearly show that interaction energies increase with the (εAl - εO) values (i.e., stronger Lewis acid-basicity pair leads to stronger interaction). It should be noted that there is a good relations between interaction energies and (εAl - εO) values for Ru_4 cluster adsorption. The parameters are 3.15 for k and -46.4 for b.

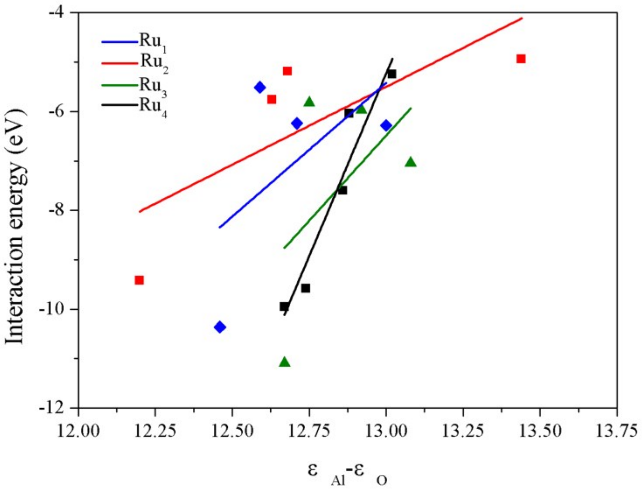

Figure S22. Interaction energies vs (εAl - εO) for the involved sites in bonding states for Ru$_n$.